



Conformational and vibrational reassessment of solid paracetamol

Ana M. Amado^{a,*}, Celeste Azevedo^b, Paulo J.A. Ribeiro-Claro^b^a Química-Física Molecular, Departamento de Química, FCTUC, Universidade de Coimbra, P-3004-535 Coimbra, Portugal^b CICECO, Departamento de Química, Universidade de Aveiro, P-3810-193 Aveiro, Portugal

ARTICLE INFO

Article history:

Received 14 December 2016

Received in revised form 11 April 2017

Accepted 26 April 2017

Available online 27 April 2017

Keywords:

Paracetamol

Quantum chemical calculations

ATR FT-IR

Raman spectroscopy

Inelastic neutron scattering

Vibrational assignments

Hydrogen bonding

ABSTRACT

This work provides an answer to the urge for a more detailed and accurate knowledge of the vibrational spectrum of the widely used analgesic/antipyretic drug commonly known as paracetamol.

A comprehensive spectroscopic analysis – including infrared, Raman, and inelastic neutron scattering (INS) – is combined with a computational approach which takes account for the effects of intermolecular interactions in the solid state. This allows a full reassessment of the vibrational assignments for Paracetamol, thus preventing the propagation of incorrect data analysis and misassignments already found in the literature. In particular, the vibrational modes involving the hydrogen-bonded N—H and O—H groups are correctly reallocated to bands shifted by up to 300 cm^{−1} relatively to previous assignments.

© 2017 Elsevier B.V. All rights reserved.

1. Introduction

The relevance and opportunity of the present work, which aims at to provide a more rigorous interpretation of the vibrational spectrum of Acetaminophen, becomes evident from the analysis of the current situation regarding the role of vibrational spectroscopy in the development of new pharmaceutical formulations.

Acetaminophen (*N*-(4-hydroxyphenyl)acetamide, commonly known as paracetamol and hereafter named as PCM; Scheme 1) is a high dose nonsteroidal anti-inflammatory drug (NSAID). It is one of the oldest and most commonly used analgesic and antipyretic drug. Though up to date, five polymorphic forms (I–V) have been identified [1–5], with the main interest being devoted to form I. This polymorph corresponds to the commercially available one, and is used in the pharmaceutical industry despite some intrinsic drawbacks, such as a very poor compressibility [6]. Co-crystallization emerges as a promising route to circumvent these intrinsic limitations of form I polymorph.

Co-crystallization is a crystallographic technique defined as bringing together, in stoichiometric amounts, two or more discrete neutral molecular species in a crystalline lattice without breaking or making covalent bonds. Stabilization is achieved due to intermolecular interactions (e.g., hydrogen, halogen and π – π interactions) established between the different molecular species [7–9]. The technique gained particular interest within the pharmaceutical industry over the last decades, as the multi-component assemblies formed may improve the physicochemical

properties of active pharmaceutical ingredients (APIs), namely aqueous solubility and/or dissolution rates, stability and bioavailability [7,8,10].

Vibrational analytical techniques, namely Raman and infrared (IR), have been increasingly implemented at different stages of drug discovery and development in the pharmaceutical industry [11–13]. When the vibrational characterization of APIs co-crystals is regarded, knowledge and understanding of the pure components, API and coformer(s), spectra is mandatory. Regarding PCM, several assignments of the vibrational spectra of the pure drug have been reported over the last decades [5,13–21]. Yet, apart from the fact that most of the assignments are very incomplete, several disagreements and inconsistencies are found. Moreover, in some cases the description of the modes is confusedly and unclearly made. Therefore, a complete reassessment of the assignments of PCM vibrational spectra is not just appropriate but also a necessary issue.

In the present work, quantum chemical calculations are used to obtain reliable information regarding the PCM conformational preferences and the magnitude of the vibrational shifts of promoted by the intermolecular interactions of the crystal lattice (e.g., hydrogen bond). The results allowed to fill the assignment gaps and to clarify the controversies encountered in the literature.

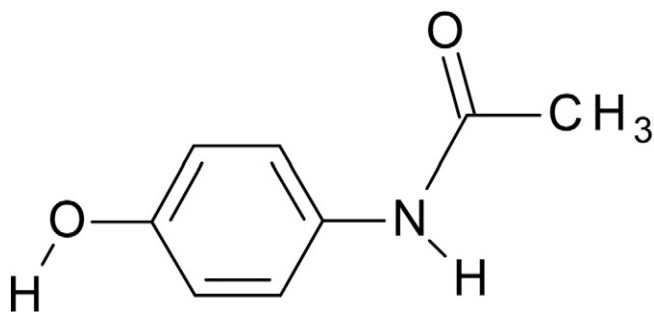
2. Experimental and Theoretical Description

2.1. Paracetamol Samples Preparation

Paracetamol was obtained commercially (Aldrich, 98%) and used without further purification. The PCM polymorphic form I was prepared as follows.

* Corresponding author.

E-mail address: amado.am@gmail.com (A.M. Amado).



Scheme 1. Schematic representation of INH.

207 mg (1.37 mmol) of paracetamol were added to 20 mL of water at 40 °C. The mixture was stirred and kept in the hot bath until complete dissolution. The obtained clear solution was allowed to slowly cool to ambient conditions and left to stand overnight. A mixture of elongated prismatic and plate-like crystals was obtained. Crystals were filtered off the solution, left to dry at ambient conditions and stored in sealed vials.

In order to help with the vibrational assignments, *N*- and *O*-deuterated crystalline samples of PCM form I were prepared following the same crystallization procedure using heavy water (D_2O ; Aldrich, 99.96%).

2.2. Vibrational Spectroscopy

2.2.1. FT-Raman Spectra

Room-temperature Fourier Transform Raman (FT-Raman) spectra were recorded on a RFS-100 Bruker FT spectrometer, using an Nd:YAG laser with an excitation wavelength of 1064 nm. Each spectrum is the average of three repeated measurements of 150 scans each. All spectra were recorded using a 2 cm^{-1} resolution.

2.2.2. ATR-FTIR Spectra

The Attenuated Total Reflection Fourier Transform Infrared (ATR-FTIR) spectra were recorded on a IFS 55 spectrometer, using a Golden Gate single reflection diamond ATR system, with no need for sample preparation. All spectra are the average of two counts of 128 scans each. A spectral resolution of 2 cm^{-1} was used in all cases.

2.3. Theoretical Calculations

Calculations were performed with the Gaussian 03w program (G03w) [22], considering the mPW1PW91 DFT combined with the widely used 6-31G* basis set, as implemented in G03 [22]. In order to evaluate the importance of the basis set size, calculations for isolated PCM molecule were also performed at the mPW1PW91/6-311++G(2d,2p) theory level. To clarify the inconsistencies found in the literature, geometry optimization and frequency calculations for the isolated molecule were further repeated using the theory levels considered in those reports (e.g., HF-6-31G, HF/6-311++G(d,p), B3PW91/6-31G*, B3PW91/6-311++G(d,p) and B3LYP/6-311++G(d,p)).

All geometries were fully optimized within the Berny algorithm, using redundant internal coordinates, and considering the G03w default convergence criteria [22]. Vibrational frequency calculations (using the *freq = raman* keyword) were performed for all optimized geometries, at the same theory level, in order to verify convergence to a real minimum within the potential energy surface (no negative eigenvalues), to infer on the magnitude of the energetic corrections (zero-point vibrational (zpve) and thermal) and to assist in the vibrational mode description. Moreover, to facilitate the identification of the vibrational modes directly associated to the NH- and OH-groups, additional calculations were performed for the amino- and hydroxyl-deuterated forms using the G03w *freq = ReadIsotopes* keyword [22]. Atomic displacements characterizing each vibrational mode were visualized using the GaussView program

[23]. Finally, in order to compare with the experimental values, calculated vibrational frequencies were corrected for anharmonicity and incomplete electron correlation treatment using the scaling factor proposed by Merrick et al. for the mPW1PW91/6-31G* theory level (0.9828 and 0.9499 for frequencies predicted below or above 500 cm^{-1} , respectively) [24].

Aiming at to estimate the effect of the intermolecular interactions in the crystal structure, mPW1PW91/6-31G* calculations were extended to molecular pairs built on the basis of the X-ray structures reported in the literature [25–28]. Prior works on the effects of the intermolecular interactions on the vibrational spectra of condensed amines proved that the mPW1PW/6-31G* theory level provides a good balance between accuracy and computational costs [29,30].

The Pairs in Molecular Materials approach (PiMM) [31] was used to correct the vibrational frequencies predicted for the isolated PCM monomer for the effects of the intermolecular interactions. This computationally-based approach for vibrational assignments circumvents the high computational cost of using a molecular cluster to model the crystal. In short, the cluster is replaced by a set of representative molecular pairs, which describe all the interactions present in the crystal. The frequency shifts predicted for the several pairs are used to correct the vibrational frequencies calculated for the isolated molecule. This approach has proven to be a reliable tool in the assignment and interpretation of the vibrational spectrum of different supramolecular systems [31–36].

Finally, in order to estimate the effect of the basis set superposition error (BSSE) on both geometry parameters and vibrational frequencies, the scheme of Boys and Bernardi [37] was used to re-optimize and recalculate the vibrational frequencies of all cluster geometries assembled. The default parameters of G03w were considered under the keyword *counterpoise* [22].

3. Results and Discussion

3.1. Conformational and Structural Analysis

3.1.1. The Isolated Molecule

Molecular structure and vibrational characterization of PCM has been the subject of several works reported during the last decades [4, 19,20,38–40]. However, crossing the results highlights several discrepancies and inconsistencies that need clarification.

Figure 1 presents the optimized molecular geometry of the four conformers predicted for isolated PCM molecule. The nomenclature used for atoms and torsional angles of free-rotation are indicated. Several other starting geometries were submitted to full optimization (Fig. S1 of the Supplementary material). These include evaluation of i) co-planarity between molecular fragments (aromatic ring, amide group and hydroxyl group), ii) *s*-cis- and *s*-trans orientation of the amide group, and iii) methyl group orientation. All those geometries were found either to converge to one of the four minima of Figure 1 or to correspond to saddle points in the potential energy surface.

Table 1 presents some selected structural parameters that characterize the four predicted minima together with their relative energy differences. Conformers presenting a symmetry plane (**M1** and **M2**) are clearly more stable than the non-planar forms **M3** and **M4**. The non-planar forms are predicted to be less stable by *ca.* $>10\text{ kJ mol}^{-1}$. In the planar forms, the amide fragment presents an *s*-trans configuration, while in the non-planar forms the *s*-cis configuration is preferred.

The lower energy minima, **M1** and **M2**, differ in the relative orientation of the hydroxyl group with respect to the amine hydrogen atom (Figure 1). This geometrical difference turns **M2** more stable than **M1** by *ca.* 1.5 kJ mol^{-1} , at the mPW1PW91/6-31G* level, after ZPVE and thermal corrections. A similar energy difference is obtained at the mPW1PW91/6-311++G(2d,2p) level. In the crystal, however, all PCM molecules present the **M1** configuration – with the OH group pointing to the same side of the NH group (*i.e.*, $\theta_1 = 0^\circ$, $\theta_2 = 0^\circ$) [25–28].

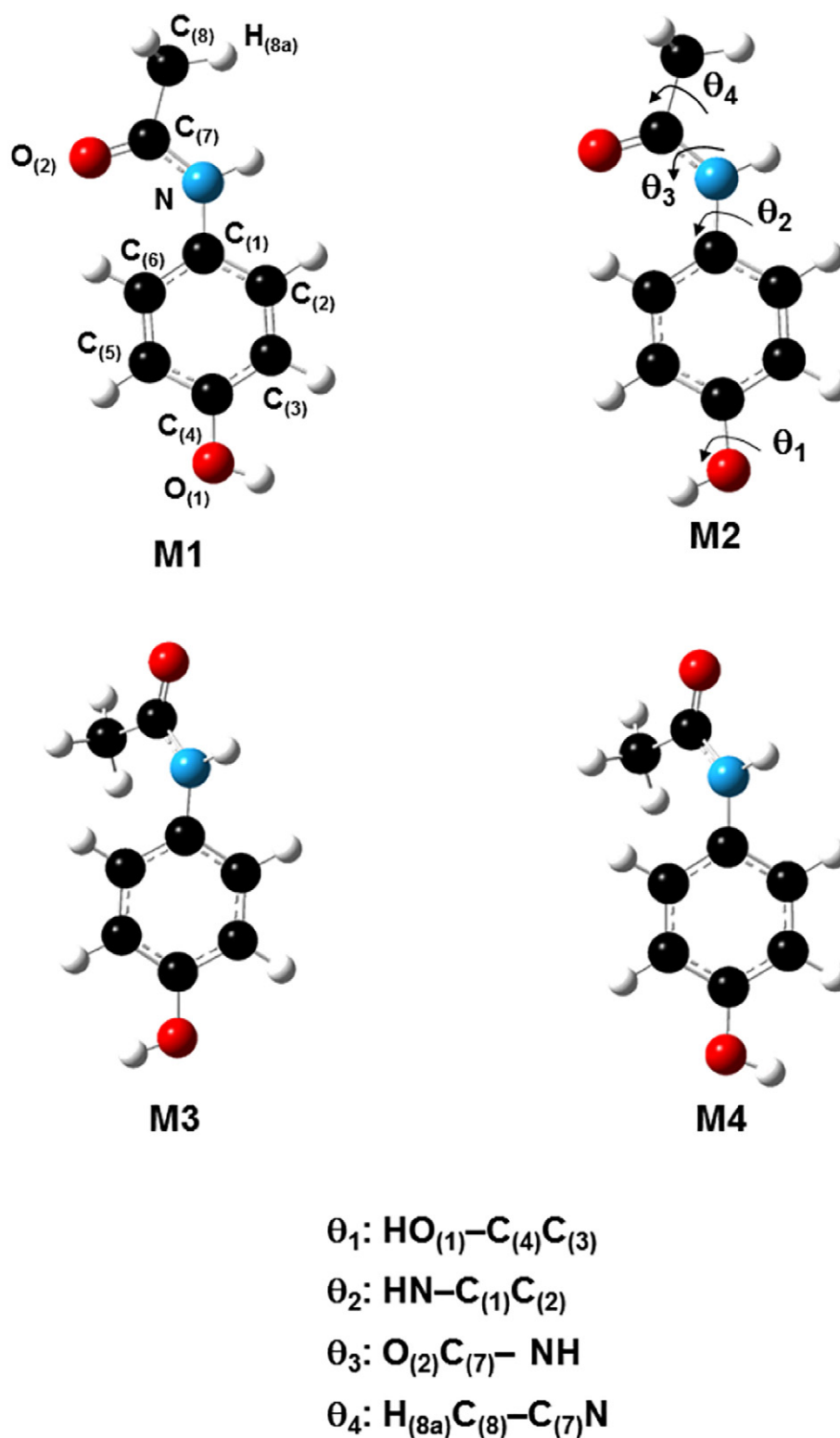


Figure 1. Optimized geometries of the four minima predicted for isolated PCM. The nomenclature used for atoms and relevant torsional angles is given.

The results concerning the relative stabilities of planar and non-planar forms are in line with the work of Oparin et al. [39], who used different DFTs (B3LYP and the newer M06) and basis sets (6-31++G(d,p) and aug-cc-pVTZ). These authors also report a similar energy difference between the two lower energy forms, but the text is not clear as to which one is the most stable. Danten et al. [19], used the B3PW91 functional combined with three basis sets of different size, to obtain conformer **M2** (no reference was made to

other possible minima, not even to **M1** conformer). This report of Danten et al. [19] is clearly incomplete, as our B3PW91/6-31G* and B3PW91/6-311++G(d,p) calculations yielded the same results as the mPW1PW91 ones.

The relative orientation of the methyl group is also matter of some controversy. In a recent work, Al-Otaibi et al. [40] used a $\theta_4 = 180^\circ$ geometry to calculate the vibrational frequencies. However, this geometry is found to present an imaginary frequency for the methyl torsional

Table 1
mPW1PW91/6-31G* relative energy differences (with and without zpve and thermal corrections) between PMol conformers and selected structural parameters.

	Conformation			
	M1	M2	M3	M4
ΔE_{rel} (kJ mol ⁻¹) ^(a)	1.7 (1.6)	0.0	12.1 (10.3)	12.1 (10.3)
zpve	1.6 (1.5)		11.6 (10.2)	11.6 (10.2)
zpve + thermal	1.5 (1.4)		10.7 (9.7)	10.7 (9.7)
Bond distances/pm				
O ₍₁₎ —H	97 (96)	97 (96)	97 (96)	97 (96)
N—H	101 (100)	101 (100)	101 (101)	101 (101)
O ₍₂₎ —C ₍₇₎	122 (121)	122 (122)	122 (122)	122 (122)
C ₍₄₎ —O ₍₁₎	136 (136)	136 (136)	136 (136)	136 (136)
C ₍₁₎ —N	141 (141)	141 (141)	141 (141)	141 (141)
Bond angles/°				
C ₍₄₎ —O ₍₁₎ —H	109 (110)	109 (109)	109 (110)	109 (110)
C ₍₁₎ —N—H	115 (115)	115 (115)	118 (118)	118 (118)
O ₍₂₎ —C ₍₇₎ —N	124 (124)	124 (124)	120 (120)	120 (120)
C ₍₈₎ —C ₍₇₎ —O ₍₂₎	121 (121)	121 (121)	122 (122)	122 (122)
C ₍₈₎ —C ₍₇₎ —N	114 (115)	115 (115)	118 (118)	118 (118)
H _(8a) —C ₍₈₎ —C ₍₇₎	115 (114)	115 (114)	113 (113)	113 (113)
Torsional angles/°				
θ_1	0 (0)	180 (180)	0 (0)	180 (180)
θ_2	0 (0)	0 (0)	−47 (−54)	−47 (−54)
θ_3	180 (180)	180 (180)	−5 (−5)	−5 (−5)
θ_4	180 (180)	180 (180)	149 (148)	149 (148)

^a Values in parenthesis are mPW1PW91/6-311++G(2d,2p) results.

mode, not only at the theory levels used in this work but also at the levels used by Al-Otaibi et al. himself [40].

When moving from the isolated molecule to the crystal, understanding of the intermolecular interactions effects is of utmost relevance. The next section evaluates and discusses those effects on the structural parameters characterizing the PCM molecule.

3.1.2. The Molecular Pairs

According to diverse X-ray reports [25–28], the crystal lattice of PCM form I polymorph (monoclinic) is composed by waved layers, presenting four molecules *per* asymmetric unit, all with a M1-like conformation (Fig. S2 (B) and (C) of the Supplementary material). Within each layer, the PCM molecules are linked via two types of strong hydrogen bonds,

namely O₍₁₎—H···O₍₂₎ and N—H···O₍₁₎ (Fig. S2 (A)). Thus, while O₍₁₎ acts simultaneously as H-bond donor and acceptor, O₍₂₎ and N act, respectively, as acceptor and donor. In order to evaluate the effects of these intermolecular interactions on the molecular structure of individual PCM units, calculations were performed for two distinct molecular pairs that mimic the two types of H-bonds revealed by the X-ray structures (O₍₁₎—H···O₍₂₎ and N—H···O₍₁₎).

Figure 2 shows the optimized geometries obtained for the two molecular pairs. These pairs are labelled **D1** (O₍₁₎—H···O₍₂₎ bonded pair) and **D2** (N—H···O₍₁₎ bonded pair) throughout the text and tables. The magnitude of some selected structural parameters (before and after cp-correction) are compared with the respective X-ray values [25–28] in Table 2. The calculated values refer to the molecular fragment being closer to the H-bond interaction.

The generality of the structural parameters is not significantly affected by cp-correction. Regarding the intramolecular structural parameters, the larger difference is observed for the θ_4 torsional angle, which is either widened or narrowed by cp-correction, depending on the molecular pair considered. In the case of the intermolecular parameters, the most significant difference is observed for the N—H···O₍₁₎ distance which is elongated upon cp-correction.

On the whole the results confirm the efficiency of the mPW1PW91/6-31G* theory level to describe the structural parameters of PCM and the intermolecular present in the crystal lattice. In fact, the calculated parameters are generally within the range defined by the different X-ray reports. The only significant exceptions refer to the θ_1 and θ_2 torsional angles, for which the calculations predict smaller values compared to the experimental ones. It is most likely that both torsional angles are pronouncedly affected by the intermolecular interactions between stacked layers, which are not accounted for in the calculations.

The next section discusses the effect of the intermolecular interactions on frequency values predicted for the fundamental modes of PCM molecule. Hydrogen-bond interactions have relevant implications in both the molecular geometry and electronic distribution, particularly in what concerns the substituents directly involved in the interactions (in the case of PCM, the acetamide and hydroxyl groups). Such effects are expected to significantly affect the fundamental vibrational modes, and cannot be ignored when analyzing the vibrational spectrum of crystalline PCM.

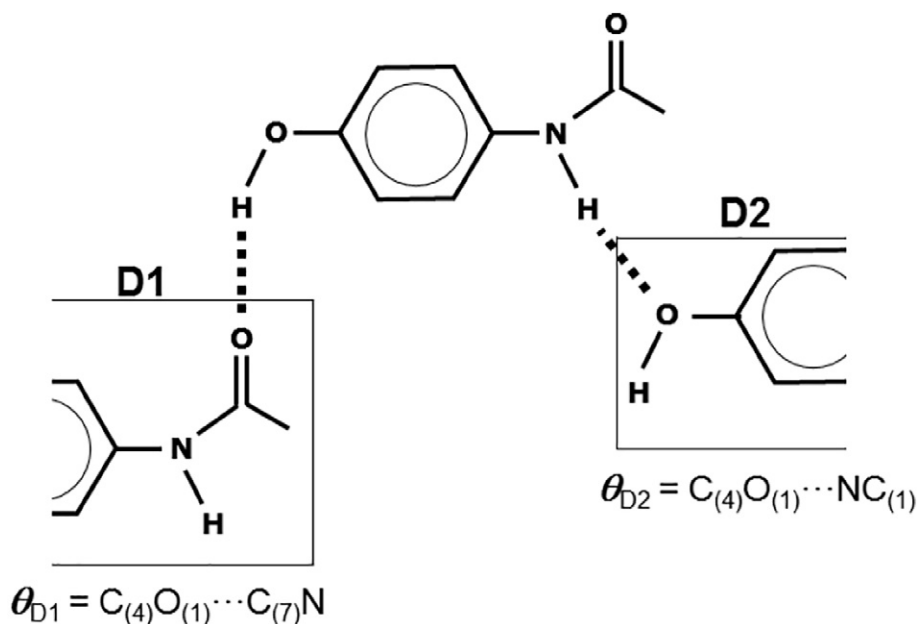


Figure 2. Schematic representation of the dimeric structures holding the PCM X-ray structure. θ_{D1} and θ_{D2} refer to the dihedral angles between molecular planes in dimers D1 and D2, respectively.

Table 2

Selected mPW1PW91/6-31G* structural parameters calculated for the dimeric PMol adducts assembled. The values predicted before and after counterpoise correction (upper and lower line, respectively) are indicated. The X-ray reported values are presented for comparison.

Parameter ^(a)	Form I					
	X-ray				mPW1PW91/6-31G*	
	Ia ^(b)	Ib ^(c)	Ic ^(d)	Id ^(e)	D1	D2
N—H	90	93	90	102	101 101	101 101
O ₍₁₎ —H	89	91	95	99	98 98	97 97
O ₍₂₎ —C ₍₇₎	123	124	124	124	123 123	122 122
C ₍₄₎ —O ₍₁₎	138	138	137	137	135 135	137 137
C ₍₁₎ —N	143	143	142	141	141 141	141 141
<i>Bond angles/°</i>						
C ₍₄₎ —O ₍₁₎ —H	109	111	111	111	110 110	109 109
C ₍₁₎ —N—H	117	115	114	113	115 115	115 115
O ₍₂₎ —C ₍₇₎ —N	123	123	123	123	123 123	125 125
C ₍₈₎ —C ₍₇₎ —O ₍₂₎	123	122	122	122	121 121	121 121
C ₍₈₎ —C ₍₇₎ —N	115	115	115	115	116 (115)	114 114
H _(8a) —C ₍₈₎ —C ₍₇₎	112	114	114	113	115 (114)	114 114
<i>Torsional angles/°</i>						
θ ₁	−19	17	19	19	−9 (1)	1
θ ₂	13	−16	−18	−18	3	8 (2)
θ ₃	−174	177	179	179	180 (−179)	178 (179)
θ ₄	−175	−168	−169	169	173 (178)	177 (173)
<i>H-bond distance/pm</i>						
(O ₍₁₎)H...O ₍₂₎	180	177	172	168	182 (181) 181	—
(N)H...O ₍₁₎	205	200	203	193	—	211 (218)
<i>H-bond angle/°</i>						
O ₍₁₎ H...O ₍₂₎	166	166	168	167	171	—
NH...O ₍₁₎	166	164	162	161	—	166
<i>H-bond torsional angle/°</i>						
θ _{D1}	85	−84	−83	−83	78	—
θ _{D2}	97	96	96	96	—	−99

^a In each case the fragment closer to the intermolecular interaction was considered.

^b (CCDC 1178859) [25].

^c (CCDC 135451) [26].

^d (CCDC 742425) [27].

^e (CCDC 754966) [28].

3.2. The Vibrational Spectra

3.2.1. Effects of the Intermolecular Interactions

The PCM molecule presents 54 normal modes of vibration, which can be described in terms of 20 bond stretching modes (ν), 14 in-plane deformation modes (α and β , from aromatic ring and substituents, respectively), 13 out-of-plane deformation modes (δ and γ , from aromatic ring and substituents, respectively), 2 torsional modes (τ) and 5 bending modes associated to the methyl group (3 deformations, δ , and 2 rockings, ρ). Visualization of the atomic displacements evidences a significant combination of oscillators for some fundamental vibrational modes. In particular, the skeletal modes related to the acetamino substituent display a very complex assignment profile. These effects may explain some (but not all) of the assignment discrepancies found in the literature.

Table 3 lists the vibrational frequencies calculated for isolated PCM molecule (**M1**) as well as the corresponding shifts resulting from the intermolecular interactions. Each vibrational shift is the arithmetic sum of

Table 3

Unscaled mPW1PW91/6-31G* vibrational frequencies (cm^{-1}) predicted for **M1** minimum (Figure 1) and corresponding assignment. The predicted vibrational shifts due to hydrogen bonding involvement (as assumed within the PiMM methodology [31]) are also listed.

Vibrational mode description ^(a)			M1	Shift
Ph ring ^(b)	Acetamino (R ₁) ^(b)	Hydroxyl (R ₂)		
		ν OH	3824	−222
ν CH	ν NH		3667	−69
ν CH			3297	+4
ν CH			3245	−7
ν CH			3212	+37
	ν_{as} CH ₃		3195	−4
	ν_{as} CH ₃		3180	+12
	ν_{s} CH ₃		3176	+6
	ν C=O		3091	+5
ν CC			1822	−43
ν CC			1713	−2
	β NH		1681	−2
ν CC			1602	+30
	δ_{as} CH ₃		1578	+1
	δ_{as} CH ₃		1523	+1
ν CC			1501	+7
	δ_{s} CH ₃		1491	+7
ν CC			1430	+2
β CH			1405	+18
ν C ₍₄₎ —R ₂			1361	+6
β CH			1335	0
ν C ₍₁₎ —R ₁			1295	+14
β CH		β OH	1271	+9
β CH			1219	+65
			1212	−1
	ρ CH ₃		1147	+2
α CCC			1067	+10
	ρ CH ₃		1041	0
γ CH			1029	+12
	ν N—C ₍₇₎ + ν C ₍₇₎ —C ₍₈₎		990	+10
γ CH			986	+2
ν CC ^(c)			912	+37
γ CH			883	−1
α CCC			863	+7
γ CH			814	+7
δ CCC			807	+24
α CCC			720	+3
	ν N—C ₍₇₎ + ν C ₍₇₎ —C ₍₈₎		662	0
	γ N—C ₍₇₎ CH ₃		636	+1
			630	−15
δ CCC			536	+2
	γ NH		528	+224
	β C=O		507	+2
β C ₍₄₎ —R ₂			431	+29
δ CCC			424	+2
β C—R ₁ + β C—R ₂			387	+2
	β N—C ₍₇₎ —CH ₃	γ OH	339	+317
			329	+5
β C ₍₁₎ —R ₁			318	+7
β C ₍₁₎ —R ₁ + β C ₍₄₎ —R ₂			188	+11
	β C ₍₁₎ —N—C ₍₇₎		158	+6
	γ C ₍₇₎ —CH ₃		79	6
	τ R ₁		48	+56
	τ CH ₃		18	+148

^a ν = stretching modes; α and β stand for in-plane deformation modes of the aromatic ring and substituents, respectively; δ and γ stand for out-of-plane deformation modes of the aromatic ring and substituents, respectively; τ = torsional modes; δ_{as} and δ_{s} stand for antisymmetric and symmetric CH₃ deformation modes; ρ = rocking modes.

^b Atom nomenclature is in accord to Figure 1.

^c Ring breathing.

the shifts predicted for each of the molecular pairs, as assumed by the PiMM methodology [31]. In the cases where significant combination of oscillators is observed, the mode descriptions given refer to the contribution involving the largest atomic displacements.

Regarding the isolated molecule, the mPW1PW91/6-31G* vibrational frequencies were found to be in very good agreement with those calculated using the 6-311++G(2d,2p) basis set (results not shown). The mean absolute deviation between the two levels is 15 cm^{-1} , and

differences do not exceed a threshold of 25 cm^{-1} , except for three vibrational modes. Namely, the νOH mode, which is 79 cm^{-1} underestimated by the mPW1PW91/6-31G* calculations and the $\nu\text{C}=\text{O}$ and γOH modes which, in turn, are overestimated by 48 and 46 cm^{-1} , respectively. However, none of these differences translates into changes of the relative vibrational modes ordering.

The effects of the intermolecular interactions are quite clear in the last column of Table 3, which lists the shifts predicted for the vibrational modes of the isolated PCM. The vibrational modes that are more pronouncedly affected are the ones associated to the molecular groups directly involved in hydrogen bonding, namely the OH and NH groups. While the νOH and νNH modes are significantly shifted to lower frequencies, the deformation modes (both β and γ) are shifted upwards. The in-plane deformations (βOH and βNH) are significantly less affected than the corresponding out-of-plane modes (γOH and γNH).

The shifts predicted for the vibrational modes related to the OH group are considerably larger than those related to the NH group. This observation correlates with the different strength of the hydrogen bonds involving both molecular groups. The $\text{O}_{[1]}\text{H}\cdots\text{O}_{[2]}$ intermolecular distance is predicted to be significantly shorter than the $\text{NH}\cdots\text{O}_{[1]}$ one (Table 2), suggesting a stronger interaction. As a result, the $\text{O}_{[1]}\text{—H}$ bond length is more affected than the N—H bond length, leading to a larger shift of the hydroxyl group related mode.

Besides the OH and NH stretching and deformation modes, the methyl torsional mode (τCH_3) is predicted to undergo a significant upward shift. Regardless of the dimeric adduct considered, the calculations predict deviations of almost 100 cm^{-1} for the τCH_3 . This considerable large shift is most likely a consequence of the close proximity of the CH_3 group to the sites of hydrogen bonding, which for sure contributes to a hindering of the torsion around of the $\text{C}_{[7]}\text{—CH}_3$ bond.

The shifts predicted for the majority of the vibrational modes are only smoothly affected by BSSE correction (results not shown). The νOH and γOH vibrational modes are again the exceptions, the shifts being considerably enhanced by BSSE correction. In what concerns the CH_3 torsional mode the opposite effect is observed, *i.e.* the predicted shifts are reduced to about one half by BSSE correction.

For the results presented, it becomes obvious that the assignment of experimental spectra based solely on calculations performed for the isolated molecule can lead to several erroneous allocations. The relative ordering of the PCM vibrational modes is considerably altered when the effects of the intermolecular interactions are accounted for (Table S1). This is particularly significant regarding the relative spectral positions of the γOH and γNH vibrational modes.

3.2.2. Assignments of the Experimental Vibrational Spectra

Figure 3 shows the room-temperature FT-Raman and ATR-FTIR spectra of crystalline PCM polymorphic form I. The spectra are similar to those reported by other authors [3,4,15,17], but present significantly better spectral resolution. Table 4 lists the experimentally observed Raman, ATR-FTIR and INS vibrational wavenumbers. The PiMM-corrected mPW1PW91/6-31G* vibrational frequencies predicted for **M1** conformer, after correction for anharmonicity and incomplete electron correlation treatment (see theoretical description section) are also included. The overall agreement between experimental and theoretical vibrational frequencies is significantly improved when both corrections are considered. The assignments presented are based on the results shown in Table 3 and are complemented with information obtained from the PCM- d_2 vibrational spectra.

As mentioned before, previous assignments are often incomplete and present disagreements and inconsistencies. The most significant controversies are discussed below.

3.2.2.1. The Region Above 3000 cm^{-1} . Most of the reported assignments ascribe the νNH and νOH vibrational modes to bands observed around 3323 and 3163 cm^{-1} , respectively [14,16–18,21]. The only exception is presented by Smith et al. [5] who report the opposite assignment based on B3LYP/6-31G** calculations for the isolated molecule. This report is a clear example of a flaw that arises from neglecting the effect of the intermolecular interactions.

The present mPW1PW91/6-31G* results on the isolated PCM (**M1** conformer) predict the νOH mode at a significantly higher frequency than the νNH mode (157 cm^{-1} apart from each other; Table 3). However, correction for the effect of the $\text{O}_{[1]}\text{H}\cdots\text{O}_{[2]}$ and $\text{NH}\cdots\text{O}_{[1]}$ hydrogen bonds places those vibrational modes nearly overlapping (3602 cm^{-1} vs. 3598 cm^{-1} ; Table 4). Considering that typically the νOH mode gives rise to broad bands [41] and that the νNH mode yields a well-defined and intense IR band, it is reasonable to assign the band observed at 3323 cm^{-1} to the νNH vibration [42,43]. The νOH mode, on the other hand, gives rise to a broad band centered around 3250 cm^{-1} , which spreads out in a wide spectral region under the 3323 cm^{-1} band. The band observed at 3162 cm^{-1} is more likely due to one of the four νCH modes of the benzene ring. In addition, the band observed around 3100 cm^{-1} is due to an overtone of the amide II band (ascribed to the coupling between the amide βNH and $\nu\text{N—C}_{(7)}$ modes), in agreement with literature reports [42,43].

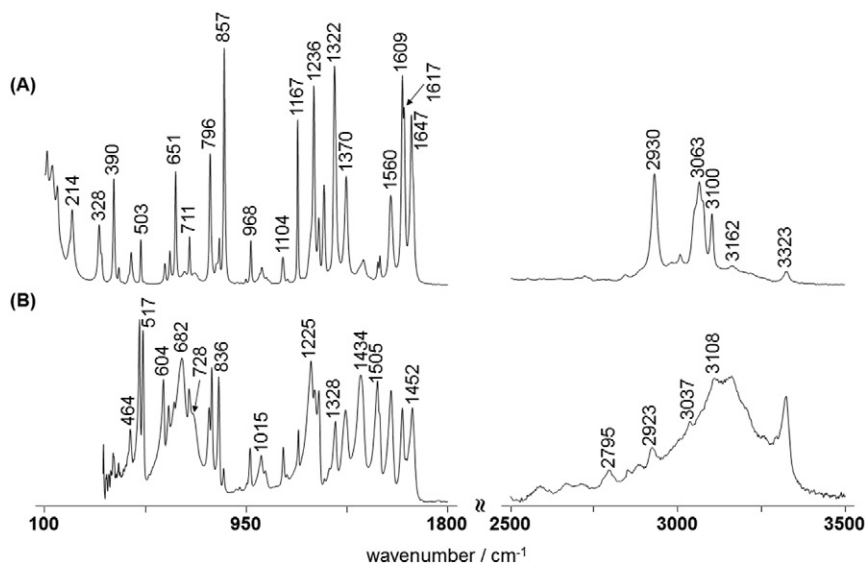


Figure 3. Experimental FT-Raman (A) and ATR-FTIR (B) spectra of solid PCM in the $100\text{--}1800\text{ cm}^{-1}$ and $2500\text{--}3500\text{ cm}^{-1}$ regions.

Table 4Assignment of the experimental FT-Raman, FTIR and INS spectra of PMol polymorphic form I based on the mPW1PW91/6-31G* calculations^(a).

Calc. ^(c)	Exp. ^(b)			Phenyl ring ^(e)	Acetamino ^(e) (R ₁)	Hydroxyl ^(e) (R ₂)
	Raman	FTIR	INS ^(d)			
3422	Very broad (≈ 3300 cm ⁻¹)					ν OH
3418	3323	3323			ν NH	
3136	3163	3160		ν CH		
	3100	3108		Fermi resonance ($2 \times \beta$ NH)		
3086	3073			ν CH		
3076	3063			ν CH		
3032	3051				ν_{as} CH ₃	
3031		3037		ν CH		
3023	3007				ν_{as} CH ₃	
2941	2930	2923			ν_s CH ₃	
	1654			Combination mode (1236 + 412)		
1690	1647	1652			ν C=O	
1625	1617	1625		ν CC		
1595	1609	1609		ν CC		
1550	1560	1561			β NH	
1500	1514	1513		ν CC		
1448	1505	1505			δ_{as} CH ₃	
1432	1444	1440			δ_{as} CH ₃	
1423	1424	1434		ν CC		
1360	1370	1371			δ_s CH ₃	
1352	1322	1328		ν CC		
1299		1303		β CH		
1268	1277	1282		ν C ₍₄₎ -R ₂		
1243	1256	1258		β CH		
1216	1236	1239		ν C ₍₁₎ -R ₁		
1220	1224	1225				β OH
1150	1167	1172	1163	β CH		
1091	1104	1108	1101	β CH		
1023	1035	1033	1027		ρ CH ₃	
989	1016	1015			ρ CH ₃	
989	1007	1008	1007	α CCC		
950	968	968		γ CH		
939	947	954	947		ν N-C ₍₇₎ + ν C ₍₇₎ -C ₍₈₎	
901		925	922	γ CH		
838	857	857	854	ν CC ^(f)		
826	834	836	835	γ CH		
780		807	806	γ CH		
789	796	796	795	α CCC		
714	731	728	747		γ NH	
687	710	712	714	δ CCC		
623	688	682	695			γ OH
629	651	649	651	α CCC		
605	627	625	622		ν N-C ₍₇₎ + ν C ₍₇₎ -C ₍₈₎	
					γ N-C ₍₇₎ CH ₃	
584	603	604	603		β C=O	
511	517	517	518	δ CCC		
475	503	502	501			
452	464	464	462	β C ₍₄₎ -R ₂		
419	412		411	δ CCC		
382	390		391	β C-R ₁ + β C-R ₂		
328	337				β N-C ₍₇₎ -CH ₃	
319	328		328	β C ₍₁₎ -R ₁		
196	214		219	β C ₍₁₎ -R ₁ + β C ₍₄₎ -R ₂		
163	150		148		τ CH ₃	
161	128				β C ₍₁₎ -N-C ₍₇₎	
102	108		106		τ R ₁	
83			91		γ C ₍₇₎ -CH ₃	

^a ν = stretching modes; α and β stand for in-plane deformation modes of the aromatic ring and substituents, respectively; δ and γ stand for out-of-plane deformation modes of the aromatic ring and substituents, respectively; τ = torsional modes; δ_{as} and δ_s stand for antisymmetric and symmetric CH₃ deformation modes; ρ = rocking modes.

^b In cm⁻¹.

^c PiMM corrected and scaled values (see text).

^d Retrieved from ISIS database [44].

^e Atom nomenclature is in accord to Figure 1.

^f Ring breathing.

3.2.2.2. The 1600 cm⁻¹ Region. The assignment of the band observed at 1560 cm⁻¹ and has been assigned to several distinct vibrational modes. In a recent study Smith et al. [5] ascribed that band to an in-plane deformation mode of the phenyl ring (α CCC). Al Zoubi et al. [15], on the other hand, assigned the same band to a stretching mode of the amide HN—C=O fragment. Several other authors correlated the band around 1560 cm⁻¹ to the β NH vibrational mode, more or less combined with other vibrational modes [13,14,16–18]. Luczak et al. [21] agreed with the assignment of Al Zoubi et al. [15] relatively to the 1560 cm⁻¹ band and claim that the β NH vibrational mode gives rise to a band at 1609 cm⁻¹.

The present results support the assignment of 1560 cm⁻¹ band to the β NH vibrational mode. Analysis of the associated atomic displacements shows that the mode is highly coupled to the ν N—C [7], in line with the description given in the literature for secondary amides (amide II) [42,43]. The disappearance of 1560 cm⁻¹ band upon deuteration, with the emergence of a new spectral feature around 1081 cm⁻¹, gives additional support to this assignment. Moreover, the 1560/1081 isotope ratio matches very well with the ratio forecasted by the mPW1PW91/6-31G* calculations. Referring to the band observed at 1609 cm⁻¹, the calculations ascribe it to one of the phenyl ν CC modes.

3.2.2.3. The 1100–1400 cm⁻¹ Region. A relevant vibrational mode expected in this region is the OH in-plane bending mode (β OH), but just a few of the reported assignments refer to it. Wang et al. [14] associate the β OH mode to a band observed at 1327 cm⁻¹, while Smith et al. [5] and Burgina et al. [17] ascribed it to the bands observed at 1123 cm⁻¹ and 1172 cm⁻¹, respectively. The present results are in disagreement with all three assignments. None of these bands was found to be affected by OH-deuteration, as it would be expected if correlated to the β OH mode.

In accord to the calculations, the bands observed around 1322 cm⁻¹, 1167 cm⁻¹ and 1104 cm⁻¹ (Table 4) are related to one ν CC and two β CH modes of the phenyl group, respectively. The β OH mode, on the other hand, is more likely related to the band observed at 1225 cm⁻¹ in the FTIR spectrum (1224 cm⁻¹ in the FT-Raman spectrum). This IR band, moderately strong as expected [41], disappears upon OH-deuteration, giving rise to a new strong IR band around 980 cm⁻¹. The corresponding 1225/980 isotope ratio is well predicted by the calculations.

3.2.2.4. The 600–800 cm⁻¹ Region. The mPW1PW91/6-31G* calculations for the isolated **M1** conformer yield the vibrational modes γ NH and γ OH at 528 and 339 cm⁻¹, respectively (Table 3). Similar values were obtained by Smith et al. [5], what prompted the assignment of those vibrational modes to the bands observed at 506 and 333 cm⁻¹. The remaining assignments found in the literature [13,18], while making no reference to the γ OH vibrational mode, assign the γ NH to a band observed around 700 cm⁻¹. This later assignment is in line with the typical value tabulated for γ NH mode, which has been described as giving rise to a broad IR band in the spectral region 650–750 cm⁻¹ [42,43].

The PiMM-corrected results predict upward shifts of 224 and 317 cm⁻¹ for the γ NH and γ OH modes, respectively (Table 3). Accordingly, the γ NH and γ OH modes predicted for isolated PCM are expected to occur around 714 cm⁻¹ and 623 cm⁻¹, respectively. Thus, it is appropriate to ascribe the γ NH and γ OH modes to the bands observed in the FTIR spectrum at 728 cm⁻¹ (Raman: 731 cm⁻¹ and INS: 747 cm⁻¹ [44]) and 682 cm⁻¹ (Raman: 688 cm⁻¹ and INS: 695 cm⁻¹ [44]), respectively (Table 4). Additional support to these assignments is obtained from the spectra of the deuterated sample. The disappearance of both spectral features is accomplished by the appearance of new bands at 548 cm⁻¹ (Raman: 546 cm⁻¹) and 446 cm⁻¹ (Raman: 448 cm⁻¹), respectively. The related 728/548 and 682/446 isotopic effects are in once again in very good agreement with the theoretical predictions.

4. Conclusions

The present study presents a thorough vibrational and quantum chemical study on paracetamol. The effects of intermolecular interactions on the prediction of the vibrational spectra were evaluated. The PiMM approach [31] was applied within the mPW1PW/6-31G* theory level, which proved to be very efficient theory level.

In accord to the X-ray reports of the literature, the crystal structure of paracetamol is hold by relatively strong $O_{[1]}-H\cdots O_{[2]}$ and $N-H\cdots O_{[1]}$ interactions besides considerably weaker inter-layer interactions. The strong intermolecular interactions were found to have a pronounced effect on the vibrational frequency of several modes. The $-OH$ and $-NH$ stretching and deformation modes were found to be particularly affected.

The reassessment of the PCM vibrational spectra assignment is clearly justified, as the prior reports, [3,4,15,17] besides being incomplete, present outstanding inconsistencies. On the light of the PiMM approach predictions, the study culminates with a full assignment of the PCM vibrational spectra. On the whole the present study stresses that full account of intermolecular interactions is an essential requisite for the interpretation of vibrational spectra based on computational simulations.

Acknowledgments

The authors acknowledge financial support from the Portuguese Foundation for Science and Technology – Unidade de Química-Física Molecular (UID/Multi/00070/2013). Acknowledgements are also due to the project CICECO – Aveiro Institute of Materials, POCI-01-0145-FEDER-007679 (FCT Ref. UID/CTM/50011/2013), financed by national funds through the FCT/MEC and when appropriate co-financed by FEDER under the PT2020 Partnership Agreement.

Appendix A. Supplementary data

Supplementary data to this article can be found online at <http://dx.doi.org/10.1016/j.saa.2017.04.076>.

References

- [1] M.A. Perrin, M.A. Neumann, H. Elmaleh, L. Zaske, Crystal structure determination of the elusive paracetamol form III, *Chem. Commun.* (2009) 3181–3183.
- [2] S. Gaisford, A.B.M. Buanz, N. Jethwa, Characterisation of paracetamol form III with rapid-heating DSC, *J. Pharm. Biomed. Anal.* 53 (2010) 366–370.
- [3] B. Zimmermann, G. Baranovic, Thermal analysis of paracetamol polymorphs by FT-IR spectroscopies, *J. Pharm. Biomed. Anal.* 54 (2011) 295–302.
- [4] L.H. Thomas, C. Wales, L.H. Zhao, C.C. Wilson, Paracetamol form II: an elusive polymorph through facile multicomponent crystallization routes, *Cryst. Growth Des.* 11 (2011) 1450–1452.
- [5] S.J. Smith, M.M. Bishop, J.M. Montgomery, T.P. Hamilton, Y.K. Vohra, Polymorphism in paracetamol: evidence of additional forms IV and V at high pressure, *J. Phys. Chem. A* 118 (2014) 6068–6077.
- [6] D.K. Bucar, J.A. Elliott, M.D. Eddleston, J.K. Cockcroft, W. Jones, Sonocrystallization yields monoclinic paracetamol with significantly improved compaction behavior, *Angew. Chem.-Int. Ed.* 54 (2015) 249–253.
- [7] N. Schultheiss, A. Newman, Pharmaceutical cocrystals and their physicochemical properties, *Cryst. Growth Des.* 9 (2009) 2950–2967.
- [8] C.C. Sun, Cocrystallization for successful drug delivery, *Expert Opin. Drug Deliv.* 10 (2013) 201–213.
- [9] A.S. Sinha, A.R. Maguire, S.E. Lawrence, Cocrystallization of nutraceuticals, *Cryst. Growth Des.* 15 (2015) 984–1009.
- [10] T. Friščić, W. Jones, Benefits of cocrystallisation in pharmaceutical materials science: an update, *J. Pharm. Pharmacol.* 62 (2010) 1547–1559.
- [11] D. Clark, The analysis of pharmaceutical substances and formulated products by vibrational spectroscopy, *Handbook of Vibrational Spectroscopy*, John Wiley & Sons, Ltd., 2006.
- [12] Applications of Vibrational Spectroscopy in Pharmaceutical Research and Development, John Wiley & Sons, Ltd., Chichester, England, 2007.
- [13] M.A. Elbagerma, H.G.M. Edwards, T. Munshi, I.J. Scowen, Identification of a new cocrystal of citric acid and paracetamol of pharmaceutical relevance, *CrystEngComm* 13 (2011) 1877–1884.
- [14] S.L. Wang, S.Y. Lin, Y.S. Wei, Transformation of metastable forms of acetaminophen studied by thermal Fourier transform infrared (FT-IR) microspectroscopy, *Chem. Pharm. Bull.* 50 (2002) 153–156.
- [15] N. Al-Zoubi, J.E. Koundourellis, S. Malamataris, FT-IR and Raman spectroscopic methods for identification and quantitation of orthorhombic and monoclinic paracetamol in powder mixes, *J. Pharm. Biomed. Anal.* 29 (2002) 459–467.
- [16] H.A. Moynihan, I.P. O'Hare, Spectroscopic characterisation of the monoclinic and orthorhombic forms of paracetamol, *Int. J. Pharm.* 247 (2002) 179–185.
- [17] E.B. Burgina, V.P. Baltakhinov, E.V. Boldyreva, T.P. Shakhshneider, IR spectra of paracetamol and phenacetin. 1. Theoretical and experimental studies, *J. Struct. Chem.* 45 (2004) 64–73.
- [18] B.B. Ivanova, Monoclinic and orthorhombic polymorphs of paracetamol-solid state linear dichroic infrared spectral analysis, *J. Mol. Struct.* 738 (2005) 233–238.
- [19] Y. Danten, T. Tassaing, M. Besnard, Density functional theory (DFT) calculations of the infrared absorption spectra of acetaminophen complexes formed with ethanol and acetone species, *J. Phys. Chem. A* 110 (2006) 8986–9001.
- [20] B.A. Kolesov, M.A. Mikhailenko, E.V. Boldyreva, Dynamics of the intermolecular hydrogen bonds in the polymorphs of paracetamol in relation to crystal packing and conformational transitions: a variable-temperature polarized Raman spectroscopy study, *Phys. Chem. Chem. Phys.* 13 (2011) 14243–14253.
- [21] A. Luczak, L.J. Jallo, R.N. Dave, Z. Iqbal, Polymorph stabilization in processed acetaminophen powders, *Powder Technol.* 236 (2013) 52–62.
- [22] M.J. Frisch, G.W. Trucks, H.B. Schlegel, G.E. Scuseria, M.A. Robb, J.R. Cheeseman, J.A. Montgomery Jr., T. Vreven, K.N. Kudin, J.C. Burant, J.M. Millam, S.S. Iyengar, J. Tomasi, V. Barone, B. Mennucci, M. Cossi, G. Scalmani, N. Rega, G.A. Petersson, H. Nakatsuji, M. Hada, M. Ehara, K. Toyota, R. Fukuda, J. Hasegawa, M. Ishida, T. Nakajima, Y. Honda, O. Kitao, H. Nakai, M. Klene, X. Li, J.E. Knox, H.P. Hratchian, J.B. Cross, V. Bakken, C. Adamo, J. Jaramillo, R. Gomperts, R.E. Stratmann, O. Yazyev, A.J. Austin, R. Cammi, C. Pomelli, J.W. Ochterski, P.Y. Ayala, K. Morokuma, G.A. Voth, P. Salvador, J.J. Dannenberg, V.G. Zakrzewski, S. Dapprich, A.D. Daniels, M.C. Strain, O. Farkas, D.K. Malick, A.D. Rabuck, K. Raghavachari, J.B. Foresman, J.V. Ortiz, Q. Cui, A.G. Baboul, S. Clifford, J. Cioslowski, B.B. Stefanov, G. Liu, A. Liashenko, P. Piskorz, I. Komaromi, R.L. Martin, D.J. Fox, T. Keith, M.A. Al-Laham, C.Y. Peng, A. Nanayakkara, M. Challacombe, P.M.W. Gill, B. Johnson, W. Chen, M.W. Wong, C. Gonzalez, J.A. Pople, Gaussian 03, Revision D.01, in: Gaussian 03, Revision D.01, Gaussian, Inc., Wallingford, CT, 2004.
- [23] R. Dennington, T. Keith, J. Millam, GaussView, Version 5, in: GaussView, Version 5, Gaussian, Inc., Shawnee Mission, KS, 2009.
- [24] J.P. Merrick, D. Moran, L. Radom, An evaluation of harmonic vibrational frequency scale factors, *J. Phys. Chem. A* 111 (2007) 11683–11700.
- [25] M. Haisa, S. Kashino, R. Kawai, H. Maeda, The monoclinic form of p-hydroxyacetanilide, *Acta Crystallogr. B* 32 (1976) 1283–1285.
- [26] G. Nichols, C.S. Frampton, Physicochemical characterization of the orthorhombic polymorph of paracetamol crystallized from solution, *J. Pharm. Sci.* 87 (1998) 684–693.
- [27] N. Bouhaida, F. Bonhomme, B. Guillot, C. Jelsch, N.E. Ghermani, Charge density and electrostatic potential analyses in paracetamol, *Acta Crystallogr. B* 65 (2009) 363–374.
- [28] Y.V. Nelyubina, I.V. Glukhov, M.Y. Antipin, K.A. Lyssenko, "Higher density does not mean higher stability" mystery of paracetamol finally unraveled, *Chem. Commun.* 46 (2010) 3469–3471.
- [29] A.M. Amado, S.M. Fiuza, L.A.E. Batista de Carvalho, P.J.A. Ribeiro-Claro, On the relevance of considering the intermolecular interactions on the prediction of the vibrational spectra of isopropylamine, *J. Chem.* 2013 (2013) 12.
- [30] S.M. Fiuza, T.M. Silva, M.P.M. Marques, L.A.E. de Carvalho, A.M. Amado, On the correction of calculated vibrational frequencies for the effects of the counterions α,ω -diamine dihydrochlorides, *J. Mol. Model.* C7–266 (21) (2015) 1–13.
- [31] M.M. Nolasco, A.M. Amado, P.J.A. Ribeiro-Claro, Computationally-assisted approach to the vibrational spectra of molecular crystals: study of hydrogen-bonding and pseudo-polymorphism, *ChemPhysChem* 7 (2006) 2150–2161.
- [32] M. Sardo, A.M. Amado, P.J.A. Ribeiro-Claro, Pseudopolymorphic transitions of niclosamide monitored by Raman spectroscopy, *J. Raman Spectrosc.* 39 (2008) 1915–1924.
- [33] M. Sardo, A.M. Amado, P.J.A. Ribeiro-Claro, Hydrogen bonding in nitrofurantoin polymorphs: a computation-assisted spectroscopic study, *J. Raman Spectrosc.* 40 (2009) 1956–1965.
- [34] M.M. Nolasco, A.M. Amado, P.J.A. Ribeiro-Claro, Effect of hydrogen bonding in the vibrational spectra of trans-cinnamic acid, *J. Raman Spectrosc.* 40 (2009) 394–400.
- [35] M.C. Costa, M. Sardo, M.P. Roelemberg, J.A.P. Coutinho, A.J.A. Meirelles, P. Ribeiro-Claro, M.A. Krähenbühl, The solid-liquid phase diagrams of binary mixtures of consecutive, even saturated fatty acids, *Chem. Phys. Lipids* 160 (2009) 85–97.
- [36] N.F.C. Mendes, M.M. Nolasco, P.J.A. Ribeiro-Claro, Effects of hydrogen-bond and cooperativity in the vibrational spectra of luminol, *Vib. Spectrosc.* 64 (2013) 119–125.
- [37] S.F. Boys, F. Bernardi, The calculation of small molecular interactions by the differences of separate total energies. Some procedures with reduced errors, *Mol. Phys.* 19 (1970) 553–566.
- [38] N. Tsapatsaris, B.A. Kolesov, J. Fischer, E.V. Boldyreva, L. Daemen, J. Eckert, H.N. Boddallo, Polymorphism of paracetamol: a new understanding of molecular flexibility through local methyl dynamics, *Mol. Pharm.* 11 (2014) 1032–1041.
- [39] R.D. Oparin, M. Moreau, I. De Walle, M. Paolantoni, A. Idrissi, M.G. Kiselev, The interplay between the paracetamol polymorphism and its molecular structures dissolved in supercritical CO_2 in contact with the solid phase: in situ vibration spectroscopy and molecular dynamics simulation analysis, *Eur. J. Pharm. Sci.* 77 (2015) 48–59.
- [40] J.S. Al-Otaibi, Vibrational (FT-IR and FT-Raman) spectroscopic studies using ab initio (HF) and DFT (B3LYP) calculations of paracetamol, *Int. J. Biol. Pharm. Allied Sci. (IJBPAAS)* 5 (2016) 887–899.
- [41] N.B. Colthup, L.H. Daly, S.E. Wiberley, Chapter 10 - ethers, alcohols, and phenols, *Introduction to Infrared and Raman Spectroscopy*, second ed. Academic Press 1975, p. 318.
- [42] N.B. Colthup, L.H. Daly, S.E. Wiberley, Chapter 9 - carbonyl compounds, *Introduction to Infrared and Raman Spectroscopy*, second ed. Academic Press 1975, p. 306.
- [43] B.H. Stuart, *Organic Molecules*, in: *Infrared Spectroscopy: Fundamentals and Applications*, John Wiley & Sons, Ltd., 2005 71–93.
- [44] <http://www.isis2.isis.rl.ac.uk/INSdatabase/>.